View Article Online
View Journal

Catalysis Science & Technology

This article can be cited before page numbers have been issued, to do this please use: L. Carneiro and A. R. Silva, *Catal. Sci. Technol.*, 2016, DOI: 10.1039/C6CY00970K.

ROYAL SOCIETY OF CHEMISTRY

www.rsc.org/catalysis

View Article Online
DOI: 10.1039/C6CY00970K

Corresponding Authors:
Dr. Ana Rosa Silva
CICECO – Aveiro Institute of Materials
Universidade de Aveiro
Campus Universitário de Santiago
3810-193 Aveiro, Portugal

Ph: +351 234 370 604
Fax: +351 234 401 470
e-mail: ana.rosa.silva@ua.pt

Selective direct hydroxylation of benzene to phenol with hydrogen peroxide by iron and vanadyl based homogeneous and heterogeneous catalysts

Liliana Carneiro, Ana Rosa Silva*

CICECO - Aveiro Institute of Materials, Department of Chemistry, University of Aveiro, 3810-193 Aveiro, Portugal. E-mail: ana.rosa.silva@ua.pt

View Article Online
DOI: 10.1039/C6CY00970K

Abstract

A series of first row transition metal complexes with Schiff base ligands or with readily available acetylacetonate ligands were screened as homogeneous catalysts in the challenging direct hydroxylation of benzene to phenol under mild conditions. Phenol was the main product of the oxidation of benzene in acetonitrile at 50°C using hydrogen peroxide as oxidant. The Fe(II/III) complexes with the Schiff base ligands were the best homogeneous catalysts using only 1% mol based on the substrate with very high selectivities. All the Fe(II/III) complexes were more selective towards phenol than the VO(IV) complexes. The Fe(II/III) Schiff base complexes were more active than the readily available Fe(II/III) acetylacetonate complexes, whereas the opposite was observed for the VO(IV) complexes. The room temperature reaction gave significantly lower phenol yield.

Due to their easy anchoring the readily available Fe(II), Fe(III) and VO(IV) acetylacetonate complexes were immobilized onto economic porous supports, hexagonal mesoporous silica and activated carbon, previously functionalized with amine groups. An Fe(III) Schiff base complex was also anchored onto these materials activated with a NaOH solution. The materials were characterized by elemental analysis, ICP-AES, FTIR, isotherms of adsorption at 77 K and TG, showing that both porous materials were conveniently functionalized and that the metal complexes could be effectively anchored onto these materials. All the heterogeneous catalysts prepared were active and selective in the direct oxidation of benzene to phenol with higher yield and selectivity than the original metal salts or complex in homogeneous phase. For the immobilized Fe(II/III) acetylacetonate complexes a significant improvement in the phenol yields were observed in comparison to the corresponding homogeneous phase catalysts, showing that the incorporation of nitrogen

DOI: 10.1039/C6CY00970K

atoms on the metal coordination sphere improves the catalytic activity. The heterogeneous catalysts could also be recycled by simple filtration and re-used at least in three more consecutive cycles without significant loss of catalytic activity. Comparable or higher phenol yields to the best reported in the literature were obtained.

Keywords: heterogeneous catalysis; homogeneous catalysis; immobilization; hydroxylation; iron; hydrogen peroxide

View Article Online
DOI: 10.1039/C6CY00970K

1. Introduction

Phenol is an important intermediate for the production of petrochemicals, agrochemicals and plastics such as phenol resins, bisphenol-A and caprolactam.[1-5] The direct oxidation of benzene is an attractive and challenging route to the synthesis of phenol. Phenol is produced industrially mainly by a three reaction step process with low phenol yields, low atomic efficiency and the formation of explosive intermediates.[1-5] This process developed in 1944 is also the most important route to acetone and due to different market for phenol and acetone much effort has been devoted to decouple their productions.[6] However, the direct one-step reaction has been often affected by low benzene conversions and/or poor selectivity, since phenol is more reactive than benzene in the oxidation process.[5] Environmentally friendly oxidants such as molecular oxygen and nitrous oxide were used, but hydrogen peroxide offers the advantage of having water as only by-product and the process is simple, green and economic.[5] Using hydrogen peroxide, heterogeneous catalysts have been mainly used such as titanosilicate molecular sieves catalysts (max. 74% benzene conversion and 86% selectivity), transition metals incorporated into molecular sieves (max. 80% benzene conversion), supported transition metal oxides on molecular sieves (max. 21% benzene conversion and 94% selectivity), complexes grafted on molecular sieves (max. 31% benzene conversion and 100% selectivity), heteropoly acids supported on molecular sieves (max. 20% benzene conversion and 95% selectivity),[5] and manganese[7a] or copper(II)[7b] tris(2-pyridylmethyl)amine complex incorporated into mesoporous silica-alumina (11% benzene conversion confirmed and 17% yield, respectively).[7a,b] Acetonitrile has been shown to be an efficient solvent for this reaction and capable of inhibiting the oxidation of phenol.[2]

View Article Online
DOI: 10.1039/C6CY00970K

The direct oxidation of benzene to phenol using homogeneous catalysts has been less explored.[8] Homogeneous catalysts based on transition metal complexes with organic ligands offer the advantage of chemoselectivity, work under mild conditions and some mimic the active centres of enzymes. Cytochrome P-450 dependant and non-heme iron-containing monooxygenases catalyse among other reactions the selective hydroxylation of aromatic compounds.[8d,e] Iron complexes with porphyrins have been being used as models for the Cytochrome P-450.[910] And several non-heme iron complexes have been being synthesized to mimic the non-heme monooxygenases, including complexes with Schiff base ligands.[8d,e,f] Unlike porphyrins,[10] Schiff base ligands can be easily synthesized with high yields from readily available chemicals, allowing great structure diversity.[9] However homogeneous catalysts are difficult to separate from the reaction media and thus they have been being supported onto porous supports in order to allow their easier recycling. If the immobilization strategy used is effective against the homogeneous catalyst leaching, this heterogeneous catalysts also hinder metal product contamination which is very important in some industries. In terms of industrial application the use of more economical and environmentally acceptable solid supports should also be preferred when preparing a heterogeneous catalyst. HMS is a type of hexagonal mesoporous silica prepared using economic alkylamines as templates, whereas conventional mesoporous silicas such as MCM-41 are prepared by strong electrostatic assembly pathways using quaternary ammonium cations as structure-directing agents.[11,12] They possess smaller particles sizes and thus short channels and large textural mesoporosity, providing better transport channels for the active centres in liquid phase catalysis.[12] Activated carbons are widely used as catalysts supports in industry and offer several advantages over inorganic porous solids.[13] Their tuneable surface chemistry, rich in oxygen functional groups, allows wider anchoring

View Article Online
DOI: 10.1039/C6CY00970K

strategies of the homogeneous catalysts than the inorganic solids, which only bear silanol groups.[14]

First row transition metal complexes are the most abundant on the surface of the earth and thus are excellent candidates to prepare economical catalysts for hydroxylation reactions. Herein we present for the first time a study on several first row transition metal complexes, some complexed with Schiff bases, as homogeneous catalysts that mediate the direct hydroxylation of benzene to phenol using hydrogen peroxide as oxidant at 50ºC in acetonitrile with very high selectivity. We also report very selective heterogeneous catalysts built by immobilization of some of the studied transition metal complexes using simple strategies. This heterogeneous catalysts could be reused at least for three cycles without loss of catalytic activity.

2. Results and Discussion

2.1. Homogeneous phase results

Although vanadyl(IV) acetylacetonate has been heterogenized into a periodic mesoporous organosilica and used as an efficient heterogeneous catalyst for the direct oxidation of benzene to phenol using hydrogen peroxide, there are lack of comprehensive studies of transition metal complexes in homogeneous phase.[3,8] The use of the most economic metals to synthesize catalysts is also preferable, such as the first row transition metals which are the most available at the crust of the earth. Therefore besides studying the catalytic activity of commercial vanadyl(IV) acetylacetonate complex in homogeneous phase, the study was extended to readily available iron(II/III) acetylacetonate complexes and several first row transition metal complexes with N_2O_2 and N_4 Schiff base ligands (Scheme 1).[9] The results

DOI: 10.1039/C6CY00970K

of using these transition metal complexes in the hydroxylation of benzene at 50°C (Scheme 2) using just 1% mol relative to benzene are compiled in Table 1 for 3 hours of reaction, using a threefold excess of hydrogen peroxide.[3]

Scheme 1 and 2, Table 1

It can be seen that all first row transition metal complexes are active in the hydroxylation of benzene. The most selective and active transition metal complex is the Fe(II) complex with the N_4 Schiff base ligand with a selectivity of 98% to phenol and 64% conversion of benzene with a turnover number (TON) of 89 in just 3 hours of reaction (Fig. S1 and S2). Elongation of the reaction time with this catalyst does not lead to better phenol yield, as the reactions are fast and are limited by the consumption/decomposition of hydrogen peroxide. The increase to 2% mol of [Fe(pyhd)Cl_2] did not lead to better phenol yield either (entry 2), as the catalyst probably increases the decomposition of hydrogen peroxide, resulting in a decrease of phenol yield. The increase of added hydrogen peroxide increases the phenol yield, and the double of the quantity leads to 77% yield of phenol instead of the 64% (entry 3). The second most active catalyst is the Fe(III) complex with the N_2O_2 Schiff base with 55% conversion of benzene and 90% selectivity towards phenol. The Fe(II) and Fe(III) acetylacetonate complexes show 96% of selectivity towards phenol, but are less active (Table 1). Thus the incorporation of nitrogen atoms in the coordination sphere of the iron centre boosts considerably the activity of the complex (Scheme 1). For the Fe(III) complexes with the N_2O_2 Schiff base, the introduction of electron-donating (Me) or electron-withdrawing groups (Br) does not improve the catalytic activity of the complex. It

View Article Online
DOI: 10.1039/C6CY00970K

is noteworthy that, with exception of [Fe(Brsalhd)Cl] with 81% selectivity, all the iron complexes tested give selectivities above or equal to 90% (Table 1). Whereas the vanadyl(IV) acetylacetonate gives 79% selectivity, which is similar to the one reported in the literature but using a ratio of benzene/catalyst 200:1, giving thus lower benzene conversion.[3] Nonetheless higher phenol yield was obtained with [VO(acac)$_2$] than with the corresponding Fe(II/III) acetylacetonate complexes. But contrary to what was observed for the iron centre, the incorporation of nitrogen atoms in the vanadyl centre decreases both the selectivity and activity of the complex (Table 1). The [Mn(salhd)Cl] and [Cu(salhd)Cl] complexes with the N_2O_2 Schiff base ligands are selective towards *p*-benzoquinone, a product of oxidation of phenol (Table 1). The [Co(salhd)Cl] complex is also highly selective towards phenol with 90% selectivity, but is less active than the corresponding Fe(III) complex. For the reactions with [VO(acac)$_2$] some experimental conditions were changed to see if the results could also be improved. The reaction performed at room temperature lowers both the benzene conversion and selectivity, thus an increase in the reaction temperature is needed in order to improve the phenol yield. The addition of nitric acid, which has a promotion effect in the oxidation of alkanes using hydrogen peroxide as oxidant and these type of homogeneous catalysts,[9] lowers slightly the selectivity (Table 1, entry 15). So there is no need for acidic co-catalysts. The addition of triphenylphosphine to the aliquot also lowers slightly the selectivity indicating that peroxide radicals are not formed in the reaction, unlike in the oxidation of alkanes using hydrogen peroxide as oxidant and these type of homogeneous catalysts (Table 1, entry 16).[9] Addition of hydrogen peroxide in one portion in the beginning of the reaction, instead of the used slow addition for one hour, also decreases slightly the selectivity towards phenol (Table 1, entry 17).[9]

DOI: 10.1039/C6CY00970K

It is noteworthy that the main by-product detected by GC-MS in the reaction was *p*-benzoquinone, formed by oxidation of phenol.[9]

The best phenol yields obtained herein were better than the recently reported Ni(II) complex with nitrogen containing ligands (21% maximum phenol yield),[8b] several non-heme iron(II) complexes[8c-f] and close to the biphasic water/acetonitrile system using iron(II) sulphate with N,O ligands and using equimolar quantity of trifluoroacetic acid as co-catalyst.[8a]

The mechanism for the oxidation of benzene using hydrogen peroxide by non-heme iron complexes has been the subject of intense research,[8c-f] but the mechanism is still a matter of debate. We did not observe biphenyl as by-product of the reaction of benzene. Thus it is indicative that the reaction does not take place through a free radical mechanism.[8c] However Fenton chemistry can not be totally ruled out, as OH radicals are able to react with benzene to give phenol[8c,d] and some radical trapping experiments lead to a small decrease in phenol yield.[8d] The fact that very high selectivities to phenol are obtained with this type of catalysts suggests that the mechanism is mainly through high valent iron species, which has also been supported by kinetic isotope effect experiments.[8c,f] Fe^{III}-OOH species have already been isolated, but studies have indicated that it decomposes by O-O bond homolysis to Fe^{IV}=O and OH radicals and by O-O bond heterolysis to Fe^{V}=O species.[8f] This last species was found to be inactive towards aromatic substrates.[8f]

Regarding the vanadyl complexes, the mechanism of the reaction is also not fully clear, but the insensitivity of the reaction towards AIBN and benzoquinone lead to the assumption that it is also a non-radical mechanism.[8g] The formation of V^{V}-OOH species has been suggested with the oxygen transfer to the benzene to proceed through a concerted mechanism.[8g]

View Article Online
DOI: 10.1039/C6CY00970K

2.2. Heterogeneous phase results

The Fe(II) and Fe(III) complexes with the Schiff base ligands were the best catalysts in homogeneous phase. However for application in industry and from a sustainable point of view a heterogeneous catalyst would be preferable due to the advantages of easy separation from the reaction media and possible recycling. The anchoring of transition metal complexes with Schiff base ligands can be complicated as often involves the change of the ligand structure in order to allow the efficient covalent attachment onto a support, which is the most effective strategy against active phase leaching. Another way is to build at the surface of the porous support the transition metal complex with the Schiff base.[3,15] As the readily available VO(IV), Fe(II) and Fe(III) acetylacetonate complexes were also active and selective in the direct oxidation of benzene to phenol they were anchored onto economic and environmentally acceptable amine functionalized activated carbon (AC) and hexagonal mesoporous silica (HMS) according to Scheme 3.a. Using this very simple immobilization procedure a Schiff base transition metal complex is formed at the surface of the porous materials by reaction of the acetylacetonate ligand with the immobilized amine groups. Nonetheless, the [Fe(salhd)Cl] complex was also immobilized onto the HMS and AC materials by direct coordination onto activated silanols and hydroxyls groups, respectively (Scheme 3.b).[16] In Table 2 are compiled the results of the elemental and ICP-AES analysis, as well as textural properties of the materials.

Scheme 3 and Table 2

View Article Online
DOI: 10.1039/C6CY00970K

The elemental analysis of the amine-functionalized materials shows the presence of nitrogen indicating that the grafting of the 3-aminopropyltriethoxysilane (APTES) onto the surface of the hexagonal mesoporous silica (HMS) and activated carbon (AC) was successful (Table 2). The HMS is able to immobilize 1.38 mmol of APTES per gram of material, whereas the AC 0.85 mmol of APTES per gram of material. Upon anchoring of the transition metal complexes, the presence of the VO(IV), Fe(II) and Fe(III) acetylacetonate complexes at the surface of the amine-functionalized AC and HMS can be confirmed by ICP-AES. The APTES@HMS is able to anchor more quantity of the [VO(acac)$_2$], [Fe(acac)$_2$] and [Fe(acac)$_3$] complexes than the APTES@AC, which might be due to the higher amount of amine groups present at the surface of the HMS than at the AC. However there is an increase of the surface area in the majority of the materials upon anchoring onto the amine-functionalized materials, which is accompanied by a decrease in the nitrogen content, which may be due to the un-efficient purification of the amine-functionalized materials (Table 2 and Fig. 1A and 1B).

By the increase in the carbon and nitrogen content observed by elemental and XPS analyse it can also be seen that the [Fe(salhd)Cl] complex was also immobilized onto the surface of activated HMS and AC (Table S1 and S2, ESI) according to Scheme 3.b. By XPS it can be further seen the presence of iron in both samples (Table S2, ESI). The immobilization process was also followed by UV-visible (Fig. S4, ESI). For the AC it can be clearly seen a decrease in the spectrum of the [Fe(salhd)Cl] complex with time, corresponding to the immobilization of the complex. And for the HMS there is a change in the spectrum of the complex, but at the end of the process the solid originally white was light orange indicating the presence of the [Fe(salhd)Cl] complex. The anchoring of the [Fe(salhd)Cl] complex

View Article Online
DOI: 10.1039/C6CY00970K

also leads to a decrease in the area of the HMS and AC materials (Table 2 and Fig. 1C and 1D).

Fig. 1

The amine-functionalization of the HMS could be further proved by the new N-H and C-H vibrations from the APTES (Fig. 2) that appear in the regions 3000-3400, 2950, 1546 and 1500-1300 cm^{-1}. Compared to this spectrum, the spectrum of the [VO(acac)$_2$]APTES@HMS material shows changes at about 2950 and 1564 cm^{-1} (Fig. 2). The shift of the last band towards higher wavenumber confirms the formation of the imine bond at the surface of the amine-functionalized material (Fig. 2). New vibration features were also observed for the [Fe(acac)$_2$]APTES@HMS and [Fe(acac)$_3$]APTES@HMS materials.[15]

The FTIR-ATR of the activated HMS is very similar to the parent material unless for a band at 968 cm^{-1}, in the region of the Si-O vibrations, which might be due to the new Si-O-Na vibrations. Upon immobilization of the [Fe(salhd)Cl] complex there is a slight shift in this band and an increase in the intensity of the band at about 1600 cm^{-1}, which might be due to the presence of the C=N band of the [Fe(salhd)Cl] complex, although it is masked by the O-H vibration of the adsorbed water.

The diffractograms for the HMS based materials were obtained and depicted in supporting information (Fig. S5 and S6, ESI), together with the corresponding d_{100} and a_0 values (Table S3, ESI). The parent HMS pattern is similar to the ones reported by Pinnavaia *et. al* for these type of materials, and the d_{100} and a_0 values are slightly lower but consistent with

View Article Online
DOI: 10.1039/C6CY00970K

the use of 1-octylamine as template.[12] Thus the pore size for the parent HMS should be around 1.6 nm.[12] After modification of the HMS either with APTES or the transition metal complexes a shift of the peak to lower angles, as well as a decrease in the intensity of peak is observed. This is usually observed upon grafting of molecules to the surface of mesoporous silicas. For the samples prepared for the immobilization of the [Fe(salhd)Cl] homogeneous catalyst, the reflux of HMS with NaOH also results in a shift of the peak to lower angles and decrease in the intensity of peak suggesting that the procedure resulted in modifications in the pore wall of the HMS. The same was observed for the material with the immobilized [Fe(salhd)Cl].

Fig. 2

The thermogravimetric curve of APTES@HMS shows a weight loss between about 200-650°C due to the decomposition of the grafted APTES in air (Fig. 3.A). The [VO(acac)$_2$] shows a sharp weight loss centred at 229ºC due to the decomposition of the acetylacetonate ligand. The [VO(acac)$_2$]APTES@HMS material shows a significantly different weight loss from APTES@HMS and [VO(acac)$_2$] suggesting the reaction between the acetylacetonate ligand of the vanadyl(IV) complex and the HMS surface amine-groups according to Scheme 3. The sharper weight loss between about 150-450°C must be due to the decomposition of the free APTES and the other between 450-600°C to the decomposition of the immobilized [VO(acac)$_2$] (Fig. 3.A).

The thermogravimetric curve of APTES@AC also shows a weight loss between about 100-450°C due to the decomposition of the grafted APTES in nitrogen (Fig. 3.B). The

View Article Online
DOI: 10.1039/C6CY00970K

[VO(acac)$_2$]APTES@AC material shows a different profile from the APTES@AC and [VO(acac)$_2$] also with two different weight losses: a smoother weight loss between about 100-350°C due to the decomposition of the APTES and another between 350-800°C where the decomposition of the immobilized [VO(acac)$_2$] must be involved (Fig. 3.B).

The thermogravimetric curve of [Fe(salhd)]@HMS shows an inflexion point around 400°C, which must be due to the immobilized complex (Fig. 3.C). The [Fe(salhd)]@AC thermogram is different from the one of AC and the sharper weight loss at higher temperature suggests the presence of the [Fe(salhd)Cl] complex (Fig. 3.D).

Fig. 3

The [VO(acac)$_2$], [Fe(acac)$_2$] and [Fe(acac)$_3$] complexes immobilized onto the amine-functionalized HMS and AC were used as heterogeneous catalysts in the hydroxylation of phenol. The results are compiled in Table 3 together with the corresponding homogeneous phase reactions.

Table 3

It can be seen that all the materials tested are active and highly selective towards the direct synthesis of phenol using hydrogen peroxide at 50°C. The immobilized [Fe(acac)$_2$] and [Fe(acac)$_3$] complexes present higher benzene conversions than the corresponding homogeneous phase reactions and thus higher phenol yields. Whereas the immobilized [VO(acac)$_2$] complex present comparable benzene conversions, but higher selectivities

View Article Online
DOI: 10.1039/C6CY00970K

towards phenol than the corresponding homogeneous phase reaction (Table 3). Therefore as observed in homogeneous phase, the incorporation of nitrogen atoms in the iron coordination sphere boosts the catalytic activity. In the case of the [VO(acac)$_2$] complex it also leads to the increase of the immobilized complex selectivity towards phenol, like reported earlier for the [VO(acac)$_2$] complex incorporated in a periodic mesoporous organosilica framework.[3] The immobilized [Fe(salhd)Cl] complex onto the HMS presents similar benzene conversion to the homogeneous phase reaction, but the phenol selectivity is also higher. Thus the immobilization of the complexes decreases the formation of over-oxidized phenol products. It is curious to note that the immobilized [Fe(acac)$_2$] complex on both HMS and AC give the best phenol yields which are comparable to the [Fe(salhd)Cl] complex immobilized onto the HMS, followed by the immobilized [VO(acac)$_2$] complex on both HMS and AC and then the immobilized [Fe(acac)$_3$] complex (Fig. 4). These materials could be further reused at least in 3 more cycles generally with comparable or even higher phenol yields and turnover numbers (Fig. 4 and Table 3).

Fig. 4

These yields reached values comparable or even higher to the ones obtained with the best homogeneous catalyst ([Fe(pyhd)Cl$_2$], entry 1 Table 1), under similar conditions, although for a higher reaction time. High selectivities were also reached by the iron complexes immobilized onto amine-functionalized activated carbon, whereas iron nitrate monohydrate impregnated on activated carbons presented comparable benzene conversions but low selectivities towards phenol (40%), reaching only 20% of phenol yield.[17] This result shows

View Article Online
DOI: 10.1039/C6CY00970K

the importance of coordination chemistry in catalysis. The anchoring of a transition metal complex onto the surface of a widely used high surface area porous support such as activated carbon is important to achieve high conversions, as well as the metal centre tuning by incorporation of other coordination atoms in the organic ligand such as nitrogen in the case of iron to achieve high selectivities.

Hence very simple, highly selective and reusable heterogeneous catalysts prepared by immobilizing readily available complexes onto amine-functionalized economic porous supports were obtained for the direct synthesis of phenol from benzene. The phenol yields obtained are higher than the ones reported for the $[VO(acac)_2]$ complex incorporated in a periodic mesoporous organosilica framework.[3] The ones for the Fe(II) and Fe(III) complexes reach the best yields reported in the literature for the titanosilicate molecular sieves catalysts (64% phenol yield)[2] and for molybdovanadophosphoric anion liquid (65% phenol yield),[18] although for higher reaction times.

3. Experimental

3.1. Materials

The reagents were used as received; 1,2-cyclohexanodiamine, salicylaldehyde, 5-bromosalicylaldehyde, 2-hydroxymethylbenzaldehyde, 2-pyridinecarboxaldehyde, iron(III) chloride hexahydrate, manganese(II) chloride dehydrate, vanadyl(IV) sulphate pentahydrate, tetraethoxysilane, 1-octylamine, (3-aminopropyl)triethoxysilane (APTES), dry toluene, benzene, vanadyl(IV) acetylacetonate, iron(II) acetylacetonate, iron(III) acetylacetonate, chlorobenzene, hydrogen peroxide 30% wt in water, nitric acid and triphenylphosphine were purchased from Sigma-Aldrich. Acetonitrile was HPLC grade and

View Article Online
DOI: 10.1039/C6CY00970K

from Romil. Ethanol was p.a. and from Merck. For the FTIR potassium bromide was used spectroscopic grade and from Sigma-Aldrich.

The starting carbon material was a NORIT ROX 0.8 activated carbon (rodlike pellets with 0.8 mm diameter and 5 mm length). This material has a pore volume of 0.695 cm^3 g$^{–1}$, as determined by porosimetry (corresponding to meso- and macropores), an ash content of 2.6% (w/w), an iodine number of 1000 and mercury and helium densities of 0.666 and 2.11 g cm$^{–3}$, respectively.

3.2. Synthesis of the ligands

The synthesis of the ligands was performed according to the process described by Holm *et al.*;[19] ethanolic solutions of salicylaldehyde, or its derivatives or 2-pyridinecarboxaldehyde, were refluxed for 1-2 hours with cyclohexanediamine in the proportion of 2:1 under vigorous magnetic stirring. Tipically, 0.015 mmol of diamine were refluxed with 0.03 mmol of salicylaldehyde in 20 ml of ethanol for one hour. The solution was kept in the freezer overnight and the precipitated ligand was collected after filtration under vacuum. All synthesized ligands were yellow and yields were between 55 and 95%.

H$_2$salhd, *N*,*N*´-bis(salicylaldehyde)-cyclohexanodiimine: $C_{20}H_{22}N_2O_2$. ^{1}H NMR (CDCl$_3$, 300 MHz, 297 K) δ/ppm: 13.5, 13.3 (s, 2H, HO), 8.4, 8.3 (s, 2H, N=CH), 7.2-7.1 (m, 4H, aromatic), 6.9-6.7 (m, 4H, aromatic), 3.6, 3.3 (m, 2H, CH$_2$), 2.0-1.5 (m, 8H, CH$_2$). EA, %: calculated C 74.51, N 6.88, H 8.69, experimental C 73.96, N 7.09, H 8.68. FTIR, ν/cm^{-1}: 2933 m, 1629 vs, 1579 m, 1280 s. UV-vis, λ_{max}/nm: 262, 357, 410.

H$_2$Brsalhd, *N*,*N*´-bis(5-bromosalicylaldehyde)-cyclohexanodiimine: $C_{20}H_{20}Br_2N_2O_2$. ^{1}H NMR (CDCl$_3$, 300 MHz, 297 K) δ/ppm: 13.4, 13.2 (s, 2H, HO), 8.3, 8.2 (s, 2H, N=CH), 7.4-7.3 (m, 4H, aromatic), 6.8 (m, 2H, aromatic), 3.6, 3.3 (m, 2H, CH$_2$), 2.0-1.5 (m, 8H,

View Article Online
DOI: 10.1039/C6CY00970K

CH_2). FTIR, ν/cm^{-1}: 2925 m, 1631 vs, 1567 m, 1475 s, 1500 m, 1280 s, 827 m.

H_2Mesalhd, *N*,*N*´-bis(5-methylsalicylaldehyde)-cyclohexanodiimine: $C_{22}H_{26}N_2O_2$. ^{1}H NMR ($CDCl_3$, 300 MHz, 297 K) δ/ppm: 13.2, 13.1 (s, 2H, HO), 8.3, 8.2 (s, 2H, N=CH), 7.1-6.9 (m, 4H, aromatic), 6.8 (m, 2H, aromatic), 3.6, 3.3 (m, 2H, CH_2), 2.3, 2.2 (m, 6H, CH_2), 1.9-1.6 (m, 8H, CH_2). FTIR, ν/cm^{-1}: 2927 m, 1631 vs, 1589 m, 1494 s, 1280 s.

pyhd, *N*,*N*´-bis(2-pyridinealdehyde)-cyclohexanodiimine: $C_{18}H_{20}N_4$. ^{1}H NMR ($CDCl_3$, 300 MHz, 297 K) δ/ppm: 8.6, 8.5 (s, 2H, N=CH), 8.3, 8.2 (m, 2H, aromatic), 7.9-7.8 (m, 4H, aromatic), 7.4 (m, 2H, aromatic), 3.7, 3.5 (m, 2H, CH_2), 1.8-1.5 (m, 8H, CH_2). ESI-HRMS, m/z: calculated ($C_{20}H_{21}N_4^+$) 293.17607, experimental 293.17618. FTIR, ν/cm^{-1}: 2927 s, 2854 s, 1644 vs, 1585s, 1564s, 1467 s, 1436 s, 788 m, 771 m.

3.3. Synthesis of the transition metal complexes

The transition-metal complexes of vanadyl(IV), manganese(III), iron(III), cobalt(III) and copper(II) were synthesized by procedures described in the literature;[19,20] equimolar solutions of ligand and metal salt (17 mmol) were refluxed for 1 to 2 hours under magnetic stirring. After precipitation of the solids they were collected by vacuum filtration and dried under reduced pressure during several days. The yields were between 49 and 62% and their structure is represented in Scheme 1.a and b. The complexes were characterized by FTIR, UV-visible, C, N and H elemental analysis and high resolution mass spectrometry.

[VO(salhd)], [*N*,*N*´-bis(salicylaldehyde)-cyclohexanodiminate] vanadyl(IV): $VC_{20}H_{20}N_2O_3$. ESI-HRMS, m/z: calculated ($VC_{20}H_{20}N_2O_3^+$) 387.09081, experimental 387.09053. EA, %: calculated C 62.02, N 7.23, H 5.20, experimental C 61.63, N 7.30, H 5.38. FTIR, ν/cm^{-1}: 2933 m, 1614 vs, 1311 s. UV-vis, λ_{max}/nm: 262, 397, 458(i), 597, ~650 (i).

View Article Online
DOI: 10.1039/C6CY00970K

[Mn(salhd)Cl], chloro-[*N*,*N*´-bis(salicylaldehyde)-cyclohexanodiminate] manganese(III): $MnC_{20}H_{20}N_2O_2Cl$. ESI-HRMS, m/z: calculated ($MnC_{20}H_{20}N_2O_2^+$) 375.08998, experimental 375.08948. FTIR, ν/cm^{-1}: 2931 m, 1621 vs, 1598 vs, 1311 s, 1278 s. UV-vis, λ_{max}/nm: 264, 412, 455 (i), ~686 (i).

[Fe(salhd)Cl], chloro-[*N*,*N*´-bis(salicylaldehyde)-cyclohexanodiminate] iron(III): $FeC_{20}H_{20}N_2O_2Cl$. ESI-HRMS, m/z: calculated ($FeC_{20}H_{20}N_2O_2^+$) 376.0869, experimental 376.0864. EA, %: calculated C 58.35, N 6.80, H 4.90, experimental C 58.34, N 6.76, H 4.99. FTIR, ν/cm^{-1}: 2937 m, 1625 vs, 1608 vs, 1311 s. UV-vis, λ_{max}/nm: 256, 475.

[Fe(Brsalhd)Cl], chloro-[*N*,*N*´-bis(5-bromosalicylaldehyde)-cyclohexanodiminate] iron(III): $FeC_{20}H_{18}N_2O_2Br_2Cl$. ESI-HRMS, m/z: calculated ($FeC_{20}H_{18}N_2O_2Br_2^+$) 531.90796, experimental 531.90549. FTIR, ν/cm^{-1}: 2937 m, 2859 m, 1644 vs, 1625 vs, 1625 vs, 1608 vs, 1460 s, 1384 s, 1314 s. UV-vis, λ_{max}/nm: 266, 394, 534.

[Fe(Mesalhd)Cl], chloro-[*N*,*N*´-bis(5-methylsalicylaldehyde)-cyclohexanodiminate] iron(III): $FeC_{22}H_{24}N_2O_2Cl$. ESI-HRMS, m/z: calculated ($FeC_{22}H_{24}N_2O_2^+$) 404.11817, experimental 404.11686. FTIR, ν/cm^{-1}: 2930 m, 2857 m, 1620 vs, 1600 vs, 1542 s, 1473 s, 1380 s, 1308 s. UV-vis, λ_{max}/nm: 266, 528.

[Co(salhd)Cl], chloro-[*N*,*N*´-bis(salicylaldehyde)-cyclohexanodiminate] cobalt(III): $CoC_{20}H_{20}N_2O_2Cl$. ESI-HRMS, m/z: calculated ($CoC_{20}H_{20}N_2O_2^+$) 379.0851, experimental 379.0846. FTIR, ν/cm^{-1}: 2935 m, 1633 vs. UV-vis, λ_{max}/nm: 256, 409, 542.

[Cu(salhd)], [*N*,*N*´-bis(salicylaldehyde)-cyclohexanodiminate] copper(II): $CuC_{20}H_{20}N_2O_2$. ESI-HRMS, m/z: calculated ($CuC_{20}H_{21}N_2O_2^+$) 384.08936, experimental 384.08908. EA, %: calculated C 62.57, N 7.30, H 5.25, experimental C 62.20, N 7.32, H 5.27. FTIR, ν/cm^{-1}: 2931 m, 1631 vs. UV-vis, λ_{max}/nm: 269, 343, 392, 552.

[Fe(pyhd)Cl$_2$], dichloro-[*N*,*N*´-bis(2-pyridinealdehyde)-cyclohexanodiminate] iron(II):

View Article Online
DOI: 10.1039/C6CY00970K

$FeC_{18}H_{18}N_4O_2Cl$. ESI-HRMS, m/z: calculated ($FeC_{20}H_{20}N_4Cl^+$) 283.07208, experimental 283.07197. FTIR, ν/cm^{-1}: 2941 m, 1651 m, 1639 m, 1597 s, 1475 m, 1448 m, 1300 m, 1036 vs, 783 s, 496 s. UV-vis, λ_{max}/nm: 265(i), 420, 520, 595(i).

3.4. Synthesis of the HMS

The HMS was synthesized according to procedures described in the literature;[11,12] tetraethoxysilane (37.0 mL, 0.166 mol) was added to a stirred solution of ethanol (88.1 mL, 1.51 mol), water (88.5 mL, 4.91 mol) and 1-octylamine (7.4 mL, 0.0448 mol). The mixture was stirred at room temperature for 24 hours. The obtained precipitate was vacuum filtered, washed with deionized water (100 mL) and ethanol (100 mL). In order to remove the template (1-octylamine), the precipitate was calcined at 600 °C for 24 hours. **HMS**: elemental analysis (%) C 0.20 H 0.16 N 0.00.

3.5. Immobilization of the [VO(acac)$_2$] onto the amine-modified HMS

A mixture of calcined HMS (5.0 g) in dry toluene (50.0 mL) and (3-aminopropyl)triethoxysilane (15.0 mmol. 3.5 mL) was refluxed for 24 hours. The material was vacuum filtered, washed with toluene (3×50 mL) and refluxed in toluene for 6 hours. The material was dried overnight in an oven at 120°C. This material will be referred as APTES@HMS (Scheme 3.a) and the loading of APTES was 1.38 mmol g^{-1} based on the nitrogen content determined by elemental analysis (46% immobilization efficiency).

The HMS functionalized with APTES (0.30 g) was added to 100 mL of a solution of [VO(acac)$_2$] (0.0400 g, 151 μmol) in toluene, and the mixture was refluxed for 20 hours. The resulting material was extensively washed with toluene and then refluxed with toluene for 24 hours and dried overnight in an oven at 120 °C, under vacuum. This material will be

DOI: 10.1039/C6CY00970K

referred as [VO(acac)$_2$]APTES@HMS (Scheme 3.a) and the loading of [VO(acac)$_2$] was 418 μmol g^{-1} based on the vanadium content determined by ICP-OES analysis (83% immobilization efficiency).

[VO(acac)$_2$]APTES@HMS: elemental analysis (%) C 8.17 H 2.37 N 1.66; ICP-AES V 2.13%, loading V 418 μmol g^{-1}.

The iron(II) and iron(III) acetylacetonate complexes were also immobilized onto the amine-modified HMS using a similar procedure. The loadings of [Fe(acac)$_2$] and [Fe(acac)$_3$] were 247 and 215 μmol g^{-1}, respectively, based on the iron contents determined by ICP-OES analysis[15] (49 and 43% immobilization efficiencies, respectively).

3.6. Immobilization of the [VO(acac)$_2$] onto the amine-modified AC

A mixture of dried AC (5.0 g) in dry toluene (50.0 mL) and (3-aminopropyl)triethoxysilane (15.0 mmol. 3.5 mL) was refluxed for 24 hours. The material was vacuum filtered, washed with toluene (3×50 mL) and refluxed in toluene for 6 hours. The material was dried overnight in an oven at 120°C. This material will be referred as APTES@AC (Scheme 3.a) and the loading of APTES was 0.85 mmol g^{-1} based on the nitrogen content determined by elemental analysis (28% immobilization efficiency).

The AC functionalized with APTES (0.60 g, respectively) was added to 200 mL of a solution of [VO(acac)$_2$] (0.0810 g, 305 μmol) in toluene, and the mixture was refluxed for 20 hours. The resulting material was extensively washed with toluene and then refluxed with toluene for 24 hours and dried overnight in an oven at 120 °C. This material will be referred as [VO(acac)$_2$]APTES@AC (Scheme 3.a) and the loading of [VO(acac)$_2$] was 418 μmol g^{-1} based on the vanadium content determined by ICP-OES analysis (43% immobilization efficiency).

View Article Online
DOI: 10.1039/C6CY00970K

$[VO(acac)_2]$APTES@AC: elemental analysis (%) C 76.24 H 2.12 N 1.08; ICP-AES (%) V 1.11; loading V 218 µmol g^{-1}.

The iron(II) and iron(III) acetylacetonate complexes were also immobilized onto the amine-modified AC using a similar procedure.[15] The loadings of $[Fe(acac)_2]$ and $[Fe(acac)_3]$ were 138 and 32 μmol g^{-1}, respectively, based on the iron contents determined by ICP-OES analysis[15] (28 and 6% immobilization efficiencies, respectively).

3.7. Immobilization of the [Fe(salhd)Cl] onto the activated HMS or AC

Firstly, the silanol and hydroxyl groups of HMS and AC (1.0 g), respectively, were activated by reflux with 100 mL of an aqueous solution of NaOH 0.01392 mol dm^{-3} for an hour. A decrease in the pH of both solutions was observed. The materials were washed with deionized water until pH 6–7 and then dried at 120°C for 6 hours, under vacuum. These materials will be designated by Na@HMS and Na@AC, respectively.

Na@HMS: elemental analysis (%) C 0.20 H 0.83 N 0.00.

Na@AC: elemental analysis (%) C 80.94 H 0.52 N 0.45.

Then 0.50 g of these materials were refluxed with 249 mL of a solution of [Fe(salhd)Cl] 4.0×10^{-4} mol dm^{-3} for 6 hours. The immobilization process was followed by UV-visible (Fig. S4) by withdrawing 1.00 mL of the solution and diluting to 5.00 mL with ethanol. The materials were filtered, washed with ethanol and then refluxed for 6 hours with 250 mL of fresh ethanol. The UV-visible spectra were also measured at the end of the process (Fig. S4). Finally, they were dried at 120°C for 6 hours, under vacuum. These materials will be designated by [Fe(salhd)]@HMS and [Fe(salhd)]@AC (Scheme 3.b), respectively, and the loading of [Fe(salhd)] was 26 and 86 μmol g^{-1} based on the variation in the %C and %N,

View Article Online
DOI: 10.1039/C6CY00970K

respectively, determined by elemental analysis (13 and 43% immobilization efficiency, respectively).

[Fe(salhd)]@HMS: elemental analysis (%) C 0.83 H 0.51 N 0.01; loading [Fe(salhd)] 26 µmol g^{-1} (variation in the %C).

[Fe(salhd)]@AC: elemental analysis (%) C 82.13 H 0.40 N 0.69; loading [Fe(salhd)] 86 µmol g^{-1} (variation in the %N).

3.8. Physicochemical Characterization

The elemental analysis (C, H and N) were done using a TruSpec 630-200-200 CNHS Analyser at University of Aveiro. The ICP-AES analysis was performed at the University of Vigo (Spain). ^{1}H NMR spectra were recorded on a Bruker Avance 300 spectrometer at 297 K, using tetramethylsilane as internal reference. Ultraviolet-visible spectra were recorded on a Jasco V-560 in the range 800-200 nm using quartz cells.

Fourier transform infrared (FTIR) spectroscopies were made in a FTIR Bruker Tensor 27 instrument. The samples were dehydrated at 110 ºC overnight before FTIR analysis.

Nitrogen adsorption-desorption isotherms were collected at -196 ºC using a Gemini V 2.00 instrument model 2380. The materials were dehydrated overnight at 120 ºC to an ultimate pressure of 1024 mbar and then cooled to room temperature preceding the adsorption.

Thermogravimetric analyses (TGA) were performed on a Shimadzu TGA-50 instrument with a program rate of 5 ºC min^{-1} in air for the HMS samples, and in nitrogen for the AC samples.

Gas chromatography experiments were performed with a Bruker 450 GC chromatograph equipped with a FID detector and using helium as carrier gas and a fused silica Varian

DOI: 10.1039/C6CY00970K

Chrompack capillary column VF-5ms (15m, 0.15 mm id, 15 mm film thickness). A Finnigan Trace GG-MS was used to confirm/identify the products.

3.9. Catalysis experiments

The oxidation of benzene was carried out in acetonitrile (ACN), at 50ºC, with constant stirring. The composition of the reaction medium was 0.040 mmol of homogeneous or heterogeneous catalyst (1% mol relative to benzene) and 4.0 mmol of benzene in 10.0 mL of ACN. The oxidant, hydrogen peroxide (1.36 mL, 12 mmol), was progressively added to the reaction medium during 1 hour using a syringe pump. Aliquots (150.0 µL) were periodically withdrawn from the reaction mixture and filtered through 0.2 µm PTFE syringe filters. Then 50.0 µl of a chlorobenzene solution in acetonitrile were added to 100.0 µl of a reaction aliquot. Other oxygenated products were identified by a Finnigan Trace GG-MS. It is noteworthy that no benzene oxidation products were detected in control experiments using the same experimental conditions, but without addition of catalyst. The heterogeneous catalysts were then filtered and washed sequentially with ACN, and dried overnight in an oven at 60 °C, under vacuum. The catalysts were then reused using the same experimental conditions. Control experiments in homogeneous phase using the metal complexes in identical reaction conditions were also performed.

4. Conclusions

Transition metal coordination compounds with very versatile and biomimetic polydentate ligands were applied as selective homogeneous catalysts in the hydroxylation of benzene under mild conditions and using environmentally benign hydrogen peroxide. The

View Article Online
DOI: 10.1039/C6CY00970K

sustainability of the homogeneous catalysts in the catalytic oxidation reactions was improved by using also economic and environmentally acceptable solid porous supports: hexagonal mesoporous silica and activated carbon. Phenol is an important intermediate for the synthesis of petrochemicals, agrochemicals, and plastics. The direct oxidation of benzene is an attractive and challenging route to the synthesis of phenol, because the industrial process involves three reaction steps. However, the direct one-step reaction is often affected by low benzene conversions and/or poor selectivity. With our homogeneous and heterogeneous catalysts very high selectivities to phenol were achieved, with yields comparable or higher to the ones reported in the literature, under mild conditions.

The developed homogeneous and heterogeneous catalysts based on first row transition metal complexes are economical and work under mild reaction conditions and could be valuable for the improvement of the sustainability and environmental impact of oxidation processes currently used in industry.

Acknowledgements

This research was supported by a Marie Curie European Reintegration Grant within the 7th European Community Framework Programme (FP7-PEOPLE-2009-RG-256509). ARS also acknowledges FCT, FSE and POPH for the contract IF/01300/2012.

References

1. L. Hu, B. Yue, C. Wang, X. Chen and H. He, *Appl. Catal. A: Gen* 2014, **477**, 141-146.

2. T. Jiang, W. Wang and B. Han, *New. J. Chem.* 2013, **37**, 1654-1664.

3. P. Borah, X. Ma, K. T. Nguyen and Y. Zhao, *Angew. Chem. Int. Ed.* 2012, **51**, 7756-7761.

View Article Online
DOI: 10.1039/C6CY00970K

4. P. K. Khatri, B. Singh, S. L. Jain, B. Sain and A. K. Sinha, *Chem. Commun.* 2011, **47**, 1610-1612.

5. W. Zhang, J. Wang, P. T. Tanev and T. J. Pinnavaia, *Chem. Commun.* 1996, 979-980.

6. L. Balducci, D. Bianchi, R. Bartolo, R. D'Aloisio, M. Ricci, R. Tassinari and R. Ungarelli, *Angew. Chem. Int. Ed.* 2003, **115**, 5087-5090.

7. (a) Y. Aratani, Y. Yamada and S. Fukuzumi, *Chem. Commun.* 2015, **51**, 4662-4665; (b) M. Yamada, K.D. Karlin and S. Fukuzumi, *Chem. Science* 2016, **7**, 2856-2863.

8. (a) D. Bianchi, R. Bortolo, R. Tassinari, M. Ricci and R. Vignola *Angew. Chem., Int. Ed.* 2000, **39**, 4321−4323; (b) Y. Morimoto, S. Bunno, N. Fujieda, H. Sugimoto and S. Itoh, *J. Am. Chem. Soc.* 2015, **137**, 5867-5870; (c) A. Raba, M. Cokoja, W.A. Herrmann and F.E. Kuhn, *Chem. Commun.* 2014, **50**, 11454-11457; (d) J.-F. Bartoli, F. Lambert, I. Morgen-stern-Badarau, P. Battioni and D. Mansuy, *C. R. Chimie* 2002, **5**, 263-266; (e) A. Thibon, J.-F. Bartoli, R. Guillot, J. Sainton, M. Martinho, D. Mansuy and F. Banse, *J. Mol. Catal. A: Chem.* 2008, **287**, 115-120; (f) O.V. Makhlynets and E.V. Rybak-Akimova, *Chem. Eur. J.* 2010, **16**, 13995-14006; (g) T.K. Si, K. Chowdhury, M. Mukherjee, D.C. Bera and R. Bhattacharyya, *J. Mol. Catal. A: Chem.* 2004, **219**, 241-247; (h) M. R. Maurya, S. Agarwal, C. Bader, M. Ebel and D. Rehder, *Dalton Trans.* 2005, 537-544.

9. A. R. Silva, T. Mourão and J. Rocha, *Catal. Today* 2013, **203**, 81-86.

10. B. Meunier, *Chem. Rev.* 1992, **92**, 1411-1456.

11. P. T. Tanev and T. J. Pinnavaia, *Science* 1995, **267**, 865-867.

12. P. T. Tanev and T. J. Pinnavaia, *Chem. Mater.* 1996, **8**, 2068-2079.

13. F. Rodriguez-Reinoso, *Carbon* 1998, **36**, 159-175.

14. J. L. Figueiredo, M. F. R. Pereira, M. M. A. Freitas and J. J. M. Órfão, *Carbon* 1999, **37**, 1379-1389.

View Article Online
DOI: 10.1039/C6CY00970K

15. A. R. Silva and J. Botelho, *J. Mol. Catal. A: Chem.* 2014, **381**, 171-178.

16. A. R. Silva, C. Freire, B. de Castro, *Carbon* 2004, **42**, 3003-3042.

17. J.-S. Choi, T.-H. Kim, K.-Y. Choo, J.-S. Sung, M.B. Saidutta, S.-O. Ryu, S.-D. Song, B. Ramachandra and Y.-W. Rhee, *Appl. Catal. A. Gen.* 2005, **290**, 1-8.

18. C. Yuan, X. Gao, Z. Pan, X. Li and Z. Tan, *Catal. Commun.* 2015, **58**, 215-218.

19. R. H. Holm, G. W. E. Everett Jr., A. Chakravorty, *Prog. Inorg. Chem.* 1966, **7**, 83-214.

20. A. R. Silva, C. Freire, B. de Castro, *New J. Chem.* 2004, **28**, 253-260.

View Article Online
DOI: 10.1039/C6CY00970K

Table 1

Catalytic hydroxylation of benzene at 50ºC with hydrogen peroxide by first-row transition metal complexes with biomimetic ligands.[a]

entry	Catalyst	Co-catalyst	%C[b]	%S[c]	%yield[d]	TON[e]
1	[Fe(pyhd)Cl_2]	none	65	98	64	89
2	[Fe(pyhd)Cl_2][f]	none	51	99	51	26
3	[Fe(pyhd)Cl_2][g]	none	77	100	77	77
4	[Fe(salhd)Cl]	none	55	90	49	51
5	[Fe(Mesalhd)Cl]	none	47	91	43	43
6	[Fe(Brsalhd)Cl]	none	32	81	26	27
7	[Co(salhd)Cl]	none	26	90	23	24
8	[VO(salhd)]	none	30	52	16	16
9	[Mn(salhd)Cl]	none	33	39	13	13
10	[Cu(salhd)]	none	26	31	8	8
11	[Fe$(acac)_2$]	none	22	96	21	19
12	[Fe$(acac)_3$]	none	20	96	19	18
13	[VO$(acac)_2$]	none	42	79	33	32
14	[VO$(acac)_2$]	HNO_3	43	75	32	30
15	[VO$(acac)_2$][h]	none	27	71	19	19
16	[VO$(acac)_2$][i]	none	44	73	32	32
17	[VO$(acac)_2$][j]	none	43	74	32	33

[a] 0.040 mmol of homogeneous catalyst (1% mol relative to benzene), 4.0 mmol of benzene, and 12.00 mmol (1.36 ml) of hydrogen peroxide as oxidant in 10.00 ml of acetonitrile in batch reactors at 50ºC and under constant stirring (1300 rpm) for 3 hours of reaction; [b] Benzene conversion, calculated by GC using the external standard method (50.0 µl of a chlorobenzene solution in acetonitrile were added to 100.0 µl of a reaction aliquot). [c] Phenol selectivity. [d] Yield based on benzene. [e] Turnover number (mmol of phenol/mmol catalyst). [f] Same reactions conditions, but using 0.0800 mmol of homogeneous (2% mol relative to benzene). [g] Same reactions conditions, but using 24.00 mmol of of hydrogen peroxide. [h] Same reactions conditions but at 25°C. [i] Same reactions conditions but PPh_3 was added to the aliquot. [j] Same reactions conditions, but hydrogen peroxide was added in one portion.

View Article Online
DOI: 10.1039/C6CY00970K

Table 2

Chemical and textural characteristics of the materials

Catalyst	**N (mmol/g)**	**Si (mmol/g)**	**M (μmol/g)**	**A_{BET} (m^2/g)**
HMS				829
APTES@HMS	1.38			119
[Fe(acac)$_2$]APTES@HMS	1.38		247	111
[Fe(acac)$_3$]APTES@HMS	1.31		215	286
[VO(acac)$_2$]APTES@HMS	1.18		418	247
AC	0.33			894
APTES@AC	0.85	0.81		525
[Fe(acac)$_2$]APTES@AC	0.94	0.85	138	562
[Fe(acac)$_3$]APTES@AC	0.85	0.75	32	632
[VO(acac)$_2$]APTES@AC	0.77		218	639
[Fe(salhd)]@HMS	0.007			301
[Fe(salhd)]@AC	0.49			873

View Article Online
DOI: 10.1039/C6CY00970K

Table 3. Heterogeneous hydroxylation of benzene at 50ºC with hydrogen peroxide and corresponding homogeneous phase reactions.[a]

entry	Catalyst	cycle	%M mol[b]	%C[c]	%S[d]	%yield[e]	TON[f]
1	[Fe(acac)$_2$]	1	1.0	33	97	32	32
2	[Fe(acac)$_2$]APTES@AC	1	1.0	53	100	53	53
3		2	1.0	70	90	63	63
4		3	0.98	65	91	59	60
5		4	0.97	62	89	55	57
6	[Fe(acac)$_2$]APTES@HMS	1	0.99	60	93	55	56
7		2	0.87	52	100	52	59
8		3	0.80	68	100	68	85
9	[Fe(acac)$_3$]	1	0.30	27	95	26	26
10	[Fe(acac)$_3$]APTES@AC	1	0.72	45	100	45	62
11		2	0.72	56	100	56	78
12		3	0.71	68	99	67	94
13		4	0.70	49	98	48	68
14	[Fe(acac)$_3$]APTES@HMS	1	0.98	46	99	46	47
15		2	0.90	46	98	45	50
16		3	0.83	45	95	43	51
17	[VO(acac)$_2$]	1	1.0	56	87	48	48
18	[VO(acac)$_2$]APTES@AC	1	0.99	56	90	50	51
19		2	0.92	50	95	48	52
20		3	0.87	61	88	54	63
21		4	0.86	61	89	54	64
22	VO(acac)$_2$]APTES@HMS	1	1.6	52	95	50	34
23		2	1.4	64	91	58	39
24		3	1.4	68	92	62	42
25		4	1.3	72	94	66	51
26	[Fe(salhd)]	1	1.0	55	90	49	51
27	[Fe(salhd)]@HMS[g]	1	0.99	54	99	54	55
28		2	0.80	64	100	64	79
29		3	0.70	39	100	39	59
30	[Fe(salhd)]@AC[h]	1	1.0	21	100	21	20
31		2	1.0	36	>99	36	36
32		3	1.0	39	97	38	58

[a] 0.040 mmol of homogeneous or heterogeneous catalyst, 4.0 mmol of benzene, and 12.00 mmol (1.36 ml) of hydrogen peroxide as oxidant in 10.00 ml of acetonitrile in batch reactors at 50ºC and under constant stirring (700 rpm) for 24 hours of reaction; [b] % mol of catalyst relative to benzene. [c] Benzene conversion, calculated by GC using the external standard method (50.0 µl of a chlorobenzene solution in acetonitrile were added to 100.0 µl of a reaction aliquot). [d] Phenol selectivity. [e] Yield based on benzene. [f] Turnover number (mmol of phenol/mmol catalyst). [g] Experiments performed using 300 mg of heterogeneous catalyst, 0.79 mmol of benzene, 1.95 ml ACN and 0.27 mmol of H_2O_2. [h] Experiments performed using 300 mg of heterogeneous catalyst, 2.59 mmol of benzene, 6.60 ml ACN and 0.90 mmol of H_2O_2.

View Article Online
DOI: 10.1039/C6CY00970K

Captions to Figures

Scheme 1 Homogeneous catalysts structure: (a) [Fe(salhd)Cl] (M=Fe, X=Cl and Y=H), [Fe(Mesalhd)Cl] (M=Fe, X=Cl and Y=Me), [Fe(Brsalhd)Cl] (M=Fe, X=Cl and Y=Br), [Mn(salhd)Cl] (M=Mn, X=Cl and Y=H), [Co(salhd)Cl] (M=Co, X=Cl and Y=H), [VO(salhd)] (M=V, X=O and Y=H), [Cu(salhd)] (M=Cu and Y=H); (b) [Fe(pyhd)Cl_2]; (c) [Fe$(acac)_2$] (M=Fe) and [VO$(acac)_2$] (M=V and Z=O); (d) [Fe$(acac)_3$].

Scheme 2 Hydroxylation of benzene to phenol.

Scheme 3 (a) Amine-functionalization of the porous materials and anchoring of the transition metal acetylacetonate complexes: [VO$(acac)_2$], [Fe$(acac)_2$] and [Fe$(acac)_3$] and (b) activation of the porous materials and anchoring of the [Fe(salhd)Cl] complex.

Fig. 1 Nitrogen adsorption isotherms at 77 K for the: (A) [VO$(acac)_2$] anchored onto amine-functionalized hexagonal mesoporous silica: (a) HMS, (b) APTES@HMS and (c) [VO$(acac)_2$]APTES@HMS; (B) [VO$(acac)_2$] anchored onto amine-functionalized activated carbon: (a) AC, (b) APTES@AC and (c) [VO$(acac)_2$]APTES@AC; (C) [Fe(salhd)Cl] anchored onto HMS: (a) HMS and (b) [Fe(salhd)]@HMS; and (D) [Fe(salhd)Cl] anchored onto AC: (a) HMS and (b) [Fe(salhd)]@AC.

Fig. 2 FTIR spectra of (a) HMS, (b) APTES@HMS, (c) [VO$(acac)_2$]APTES@HMS and (d) [VO$(acac)_2$]; and FTIR-ATR spectra of: (a) HMS, (b) Na@HMS and (c) [Fe(salhd)]@HMS.

View Article Online
DOI: 10.1039/C6CY00970K

Fig. 3 Thermograms for the: (A) [VO(acac)$_2$] anchored onto amine-functionalized hexagonal mesoporous silica, (B) [VO(acac)$_2$] anchored onto amine-functionalized activated carbon, (C) [Fe(salhd)Cl] anchored onto the activated HMS and (D) [Fe(salhd)Cl] anchored onto the activated AC.

Fig. 4 % phenol yield in function of the catalyst used.

View Article Online
DOI: 10.1039/C6CY00970K

Scheme 1

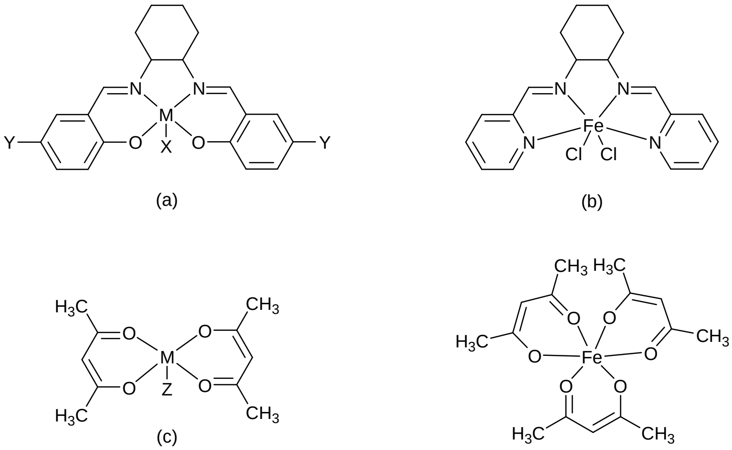

(a) (b)

(c) (d)

View Article Online
DOI: 10.1039/C6CY00970K

Scheme 2

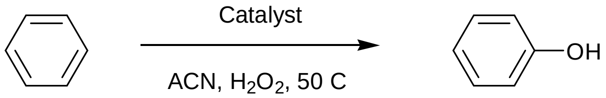

View Article Online
DOI: 10.1039/C6CY00970K

Scheme 3

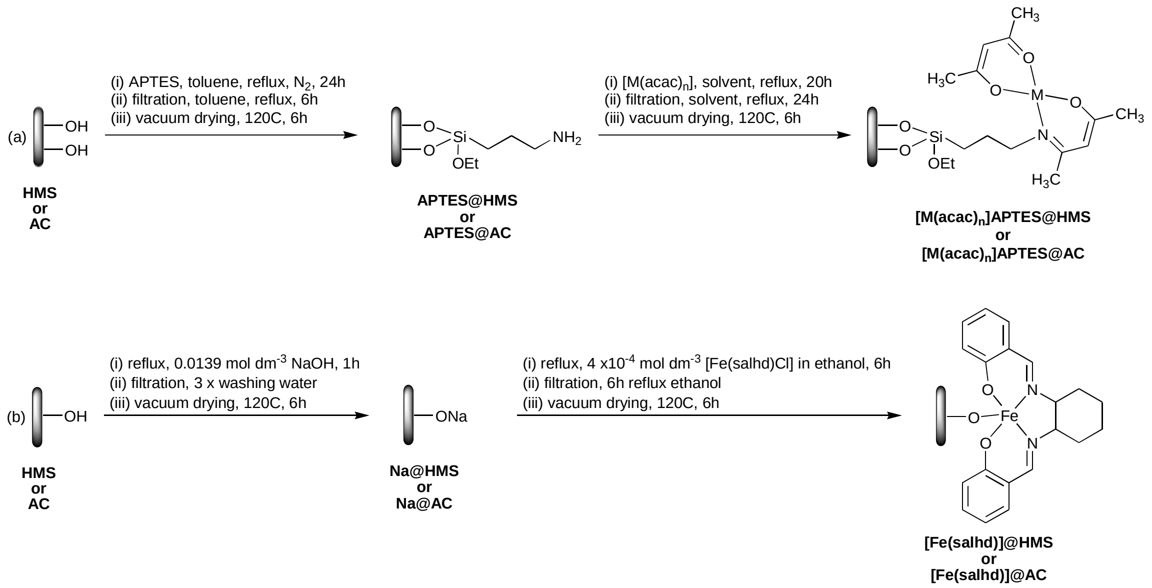

View Article Online
DOI: 10.1039/C6CY00970K

Fig. 1

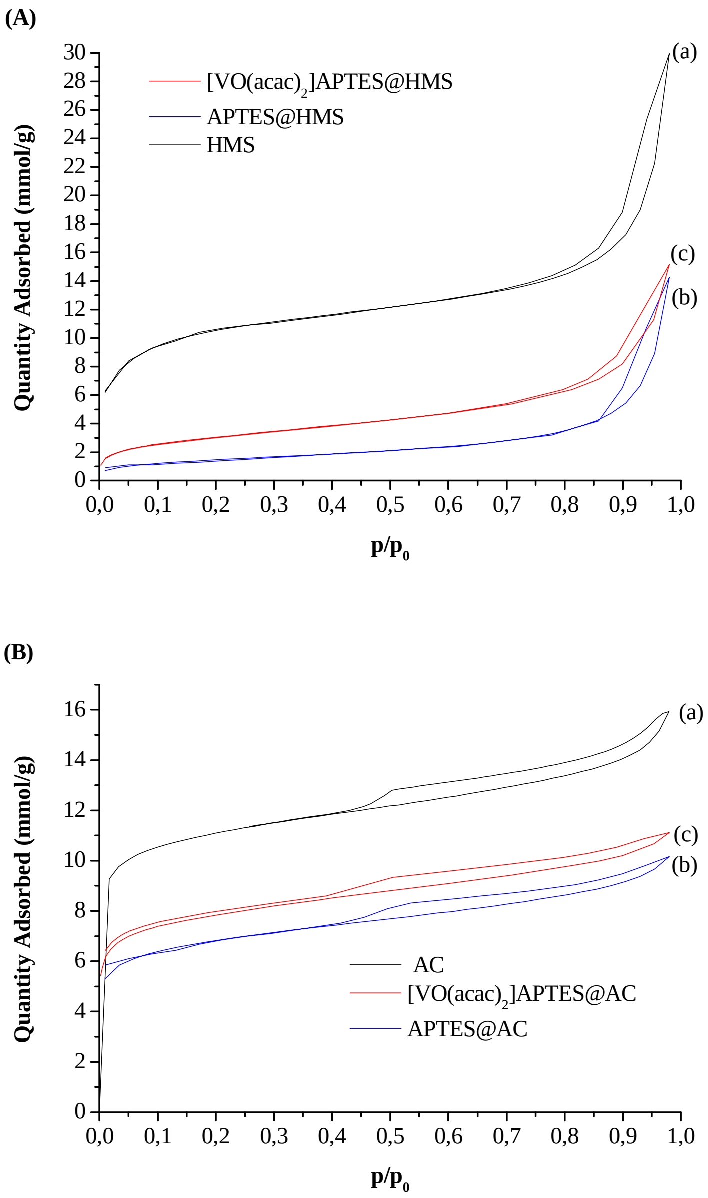

View Article Online
DOI: 10.1039/C6CY00970K

(C)

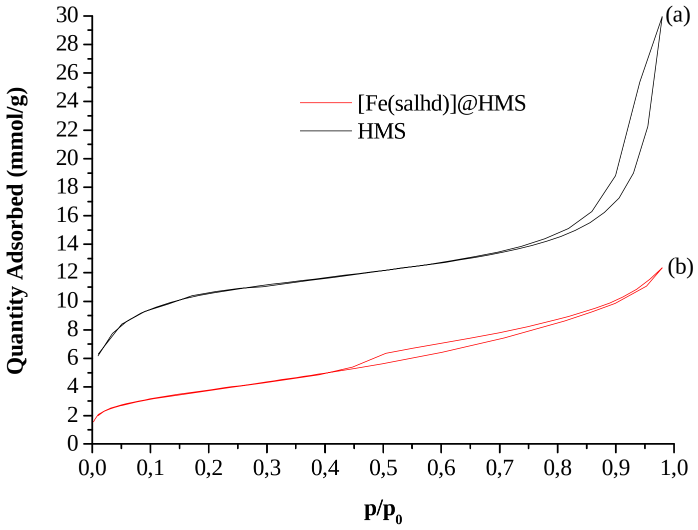

(D)

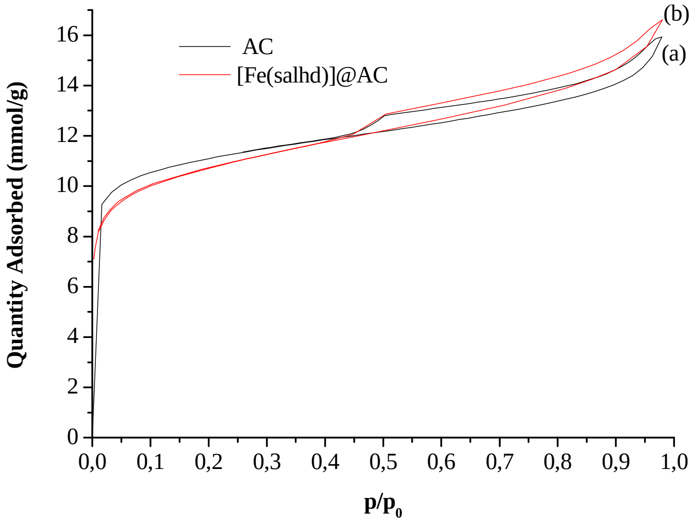

View Article Online
DOI: 10.1039/C6CY00970K

Fig. 2

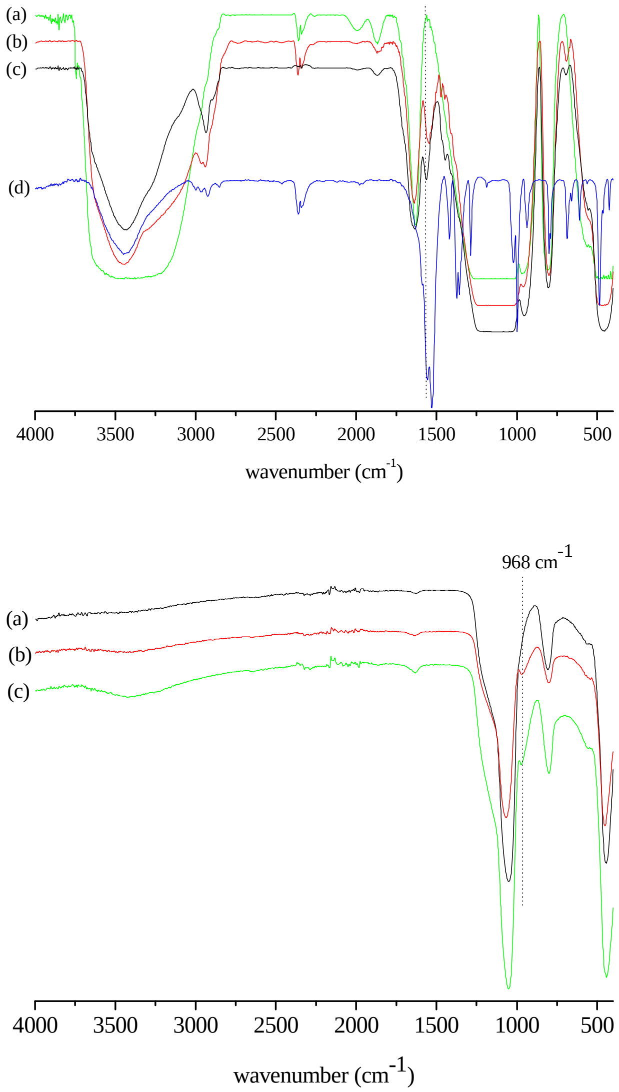

View Article Online
DOI: 10.1039/C6CY00970K

Fig. 3

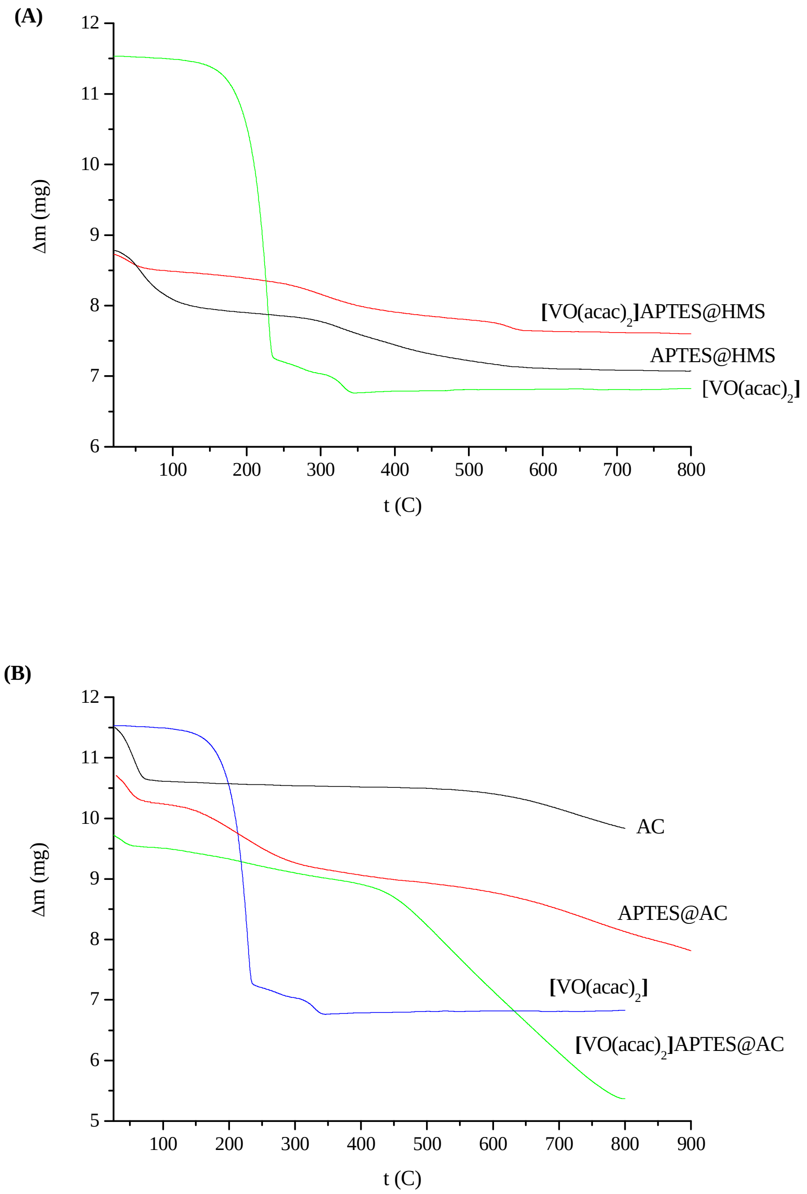

View Article Online
DOI: 10.1039/C6CY00970K

(C)

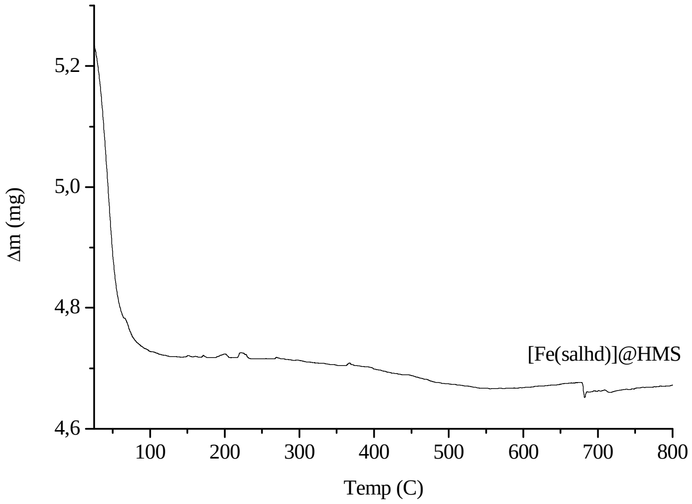

(D)

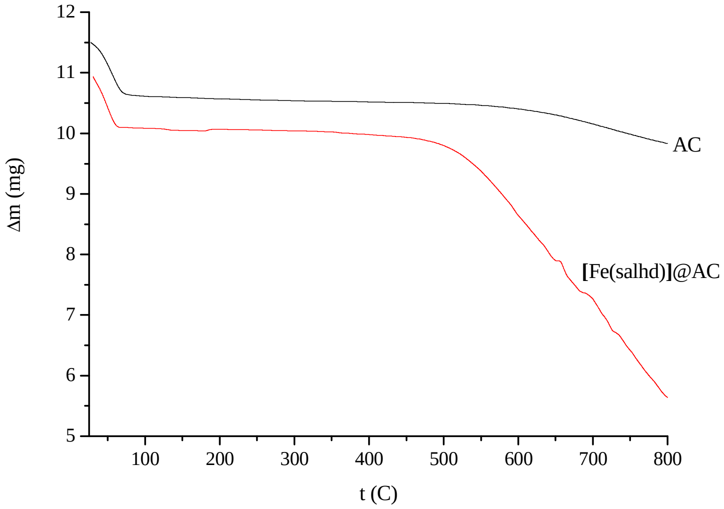

View Article Online
DOI: 10.1039/C6CY00970K

Fig. 4

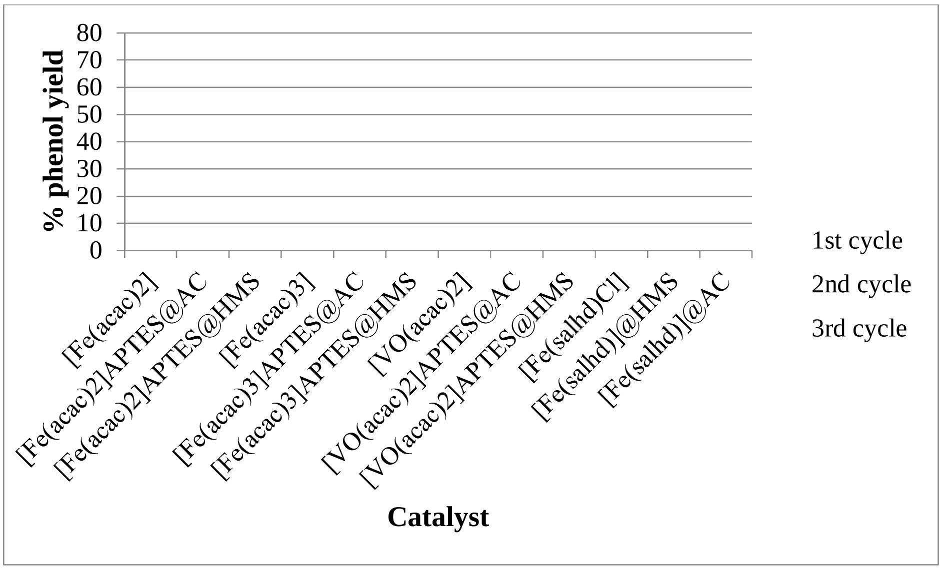

View Article Online
DOI: 10.1039/C6CY00970K

Graphical abstract

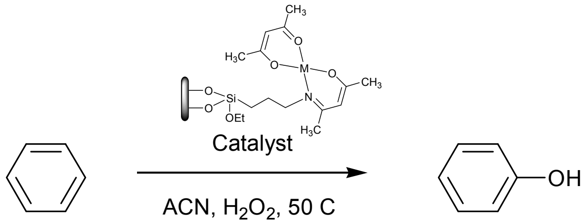

With our homogeneous and heterogeneous catalysts very high selectivity to phenol was achieved, with yields comparable or higher to the ones reported in the literature, under mild conditions.